

Kinematics and Dynamics of Machines - MIE 301

Design Final Report on Wheeled Leg Jumping Robot

Team Name: 30G Worx

1. Han Hu 1008797553
2. Yuyang Gao 1008758952
3. Fanzhen Kong 1008959192
4. Jiajin Yuan 1008786397
5. Kai Zhang 1008720902

Date Report Submitted: December 8th, 2024

1.0 Introduction

In the rapidly evolving technology of robotics, the development of robots gives people a leap forward in how machines automate tasks, increase efficiency, and enhance safety. The client, Global Response Innovations (GRI), is a government-funded agency with a mandate to improve disaster response capabilities worldwide. In recent years, GRI has recognized significant difficulty in their capabilities related to urban search and rescue operations, particularly in densely populated areas where debris and structural collapses are prevalent. Now, GRI is looking for a new prototype robot that would not only scout disaster zones quickly and efficiently but also carry sensors and supplies, making it an essential part of their future rescue missions. This proposal will aim to provide a solution for the proposed problem and provide analysis techniques as methods of justification for the project.

2.0 Literature Review

This section will provide justification for the project both by studying the application scenarios of the device and investigating the technical feasibility of the project by referencing pre-existing literature.

2.1 Statement of Purpose

The purpose of this project is to design a robot capable of navigating complex terrain environments effectively. When comparing the two main categories of current robot designs, wheeled robots struggle with obstacles larger than twice the wheel diameter, while legged robots, despite having very complex locomotion systems both in control algorithms and the legs structures, are generally more adept at navigating rough terrain [1]. Therefore, a design that combines both the high energy efficiency of wheels on flat surfaces with the adaptability of legs for rough and uneven terrain is required. As the research group identified, jumping is the most efficient way for small sized robots to travel over very rough terrain, a method also commonly used by many natural organisms to navigate such challenging environments.

2.2 Previous Design

The project's technical feasibility is well-supported by existing literature, highlighting the advantages of hybrid locomotion systems that combine wheeled speed and stability with legged adaptability. Wheels excel on flat surfaces but struggle with high obstacles, while legs offer adaptability at the cost of speed and efficiency. By integrating these strengths, the hybrid design ensures efficient, versatile movement, ideal for navigating complex terrains.

In the article "*Design and Implementation of a Two-Wheel and Hopping Robot With a Linkage Mechanism*", a mechanism for a plumbing robot using a floating four-bar mechanism is introduced [2], where instead of fixating one element as a reference, the design only fixates one joint such that a two degree of freedom motion can be achieved. The following figure shows a simplified kinematic model of the leg mechanism and the detailed model.

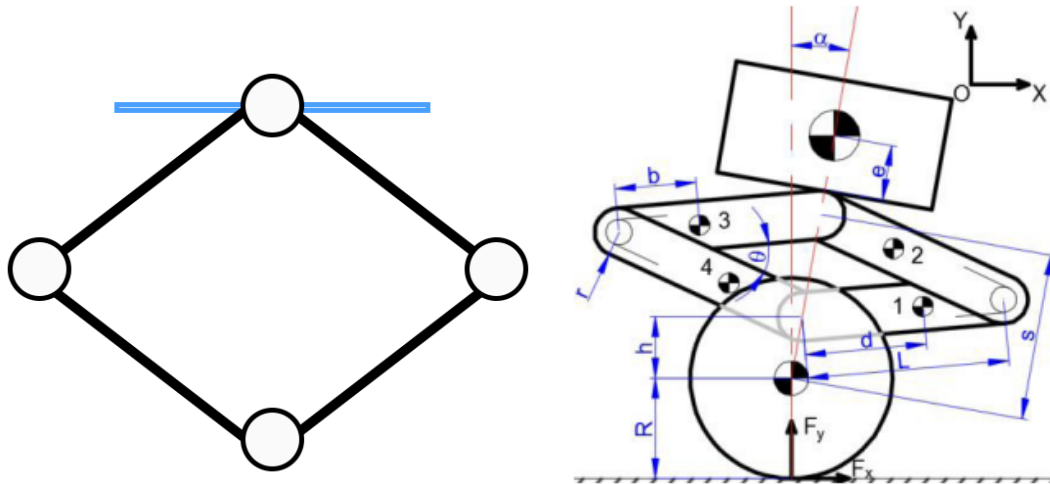


Figure 1. Previous Design of Jumping Robot

Since this report mainly concerns the analysis of the mechanisms on the leg, only the dimensions of element length, L , will be considered. According to the paper, all elements have the same length of 50mm [2]. After simulation is conducted on this device, it is found that the robot is capable of reaching an initial jump velocity of 1.66 m/s and heights over 120 mm. These results highlight the system's efficiency, adaptability, and readiness for real-world deployment, offering a strong foundation for leveraging similar mechanisms in this project.

However, developing wheel-legged robots presents several challenges. A key issue is the high cost of advanced technologies, such as Field-Oriented Control (FOC) brushless motors, which can exceed CAD 150 per unit and significantly increase costs when scaled for larger applications [3]. Structural and control complexities also persist; energy storage and release mechanisms, like torsional springs, often face synchronization issues during takeoff and landing, leading to unstable trajectories. Additionally, optimizing control algorithms for smooth transitions between wheeled and jumping modes is crucial to improving robustness and minimizing failure risks during high-impact maneuvers. These challenges highlight the trade-offs between functionality, cost, and reliability, emphasizing the need for innovative solutions to overcome these limitations.

Considerations on the jumping height are also ought to be re-evaluated. While the height of 120mm is suitable for application in selective scenarios, applications in other scenarios requiring an upscaled design of the similar concept would need a different set of simulations to verify the feasibility of the project.

In conclusion, the proposed wheeled-leg jumping robot proves feasible with its hybrid locomotion, efficient mechanisms, and reliable control systems. Despite challenges, it shows potential for applications in search-and-rescue, exploration, and logistics. In the new design, studies will primarily focus on analyzing the feasibility of upscaling the design to achieve both a higher jump while maintaining a reasonable cost expectation.

3.0 Methods and Findings

This section aims to discuss the detailed mechanism of the jumping mechanism. A kinematic model and its corresponding method of analysis will also be proposed in this section.

3.1 Mechanism Overview

To actively achieve balancing and jumping in the same mechanism, a 2 Degrees of Freedom (DoF) system is needed, thus for the actual mechanism, a device similar to the discussed literature is designed and shown in figure 2. In both the proposed literature and this design, the ground element is directly connected to two other elements via a riveted joint. While the literature uses more custom designs of motors to achieve coaxial movement in the two bars, this design introduces offset to better adapt to cheaper off-the-shelf motors. Figure 2 is a CAD model of the design, where the black boxes with blue stickers are input to linkages.

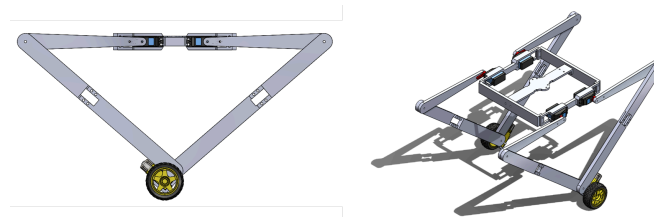


Figure 2. CAD Model of Mechanism[4] [5] [6]

Figure 3 below shows a kinematic model for the new mechanism. Notice how both the devices shown in figure 1 and figure 3 are 2 DoF systems.

5 Elements: 1-5.

5 Riveted Joints: (1,2), (1,3) (2,4) (3,5) (4,5);

$$DoF = 3 \times (5 - 1) - 2 \times 5 = 2$$

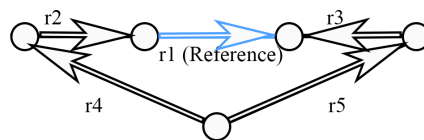


Figure 3. Kinematic Models of Proposed Device (Right)

The new design follows the following specifications in table 1.

Table 1. Detailed specifications for the mechanism

Element	Data:
θ_2, θ_3	38.0 kgcm at 7.4V; [4] No Load (Maximum) Speed 0.11sec/60deg [4]
r1	12cm
r2, r3	23cm
r4, r5	36cm

In the device, the rotational input on joints (1,2), and (1,3) will rotate the elements to create linear transformation on joints (4,5) to create an upward motion to achieve a jump. Wheels will be assumed to be installed on joints (4,5) for the purpose of the analysis. In practice, a small offset would create a similar approach. In the improved design this design group (30G Worx) proposed, an off the shelf servo motor [4] is integrated with a jumping mechanism with the following mechanism to form a primitive prototype for the leg linkages shown in figure 4.

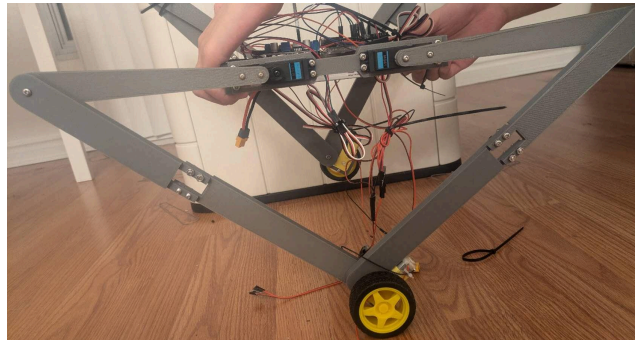


Figure 4. Photo of Proposed Prototype Linkages

3.2 Simplification to Mechanism for Analysis on Jumping Motion

In this case, both θ_2 and θ_3 are inputs to consider. To simplify this mechanism such that analysis techniques in the scope of MIE301 can be applied the following assumptions were made.

The jumping motion will be investigated separately from stability control to simplify physics calculation. During a jump, the joint (4,5) is expected to move horizontally downwards. Thus we can assume that joint (4,5) will always be at a given x value for this part of the analysis.

For linear motion analysis of the robot, we will show that the sum of moment with respect to the center of mass can be controlled by all inputs by drawing the mechanism in all three states of:

- Acceleration,
- Steady motion, and
- Deceleration

In each case, to simplify both the control algorithm and the analysis, three methods to control the linkages will be considered, they are:

- Moving θ_2 and fixing θ_3
- Moving θ_2 and fixing θ_3
- Moving θ_2 and θ_3 with the same offset.

3.3 Fundamental Motion Simulations

To further study the system, a numerical model is constructed for all the simulation cases discussed above. The assumption in the previous section can then be written in the following numeric form. The objective for both scenarios (jumping/stability) of analysis will also be different. All objectives for analysis are shown in table 2 categorized by the different motions.

3.3.1 Jumping Motion

For the purpose of simplifying calculation, we assume that the mass of the legs ($\sim 10\text{g}$ each) is negligible when compared to the main body of the robot ($r1$) that holds all the electronics ($\sim 2\text{kg}$ when accounting for all electronics onboard). To calculate the jump height, departing velocity needs to be found first. To do so, a set of equations that uses the torque on the motor to compute vertical forces will be made and solved. The following free body diagram can be constructed.

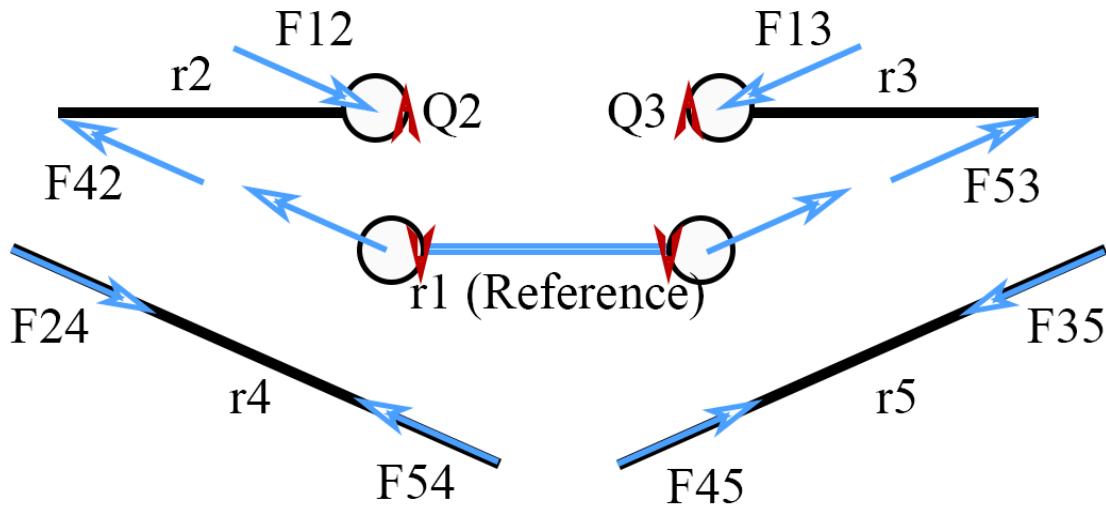


Figure 5. Detailed Free Body Diagram with Internal Forces

Notice how $F45$ and $F54$ are forces that have an equal vertical component and an equal and opposite horizontal component. This is because it was assumed in the previous section that the motor on both the arms behave the same, thus it is safe to assume that element 5 is a mirror of element 4. It can also be said that the lowest joint remains stationary with respect to ground during the acceleration before the jump, and thus the simplification can be made that the total vertical force exerted to the mass of this system, F_y is 2 times of the internal force pointing upward in one of the elements. Solve for the vertical force using the free body diagram drawn above and times 2 for total vertical force applied onto the system. Figure 6 below shows the equivalent external force as a result of the motor action, minus F_y by force due to gravity and divide this total force by mass of 2kg for acceleration, and integrate analytically once for velocity, twice for position.

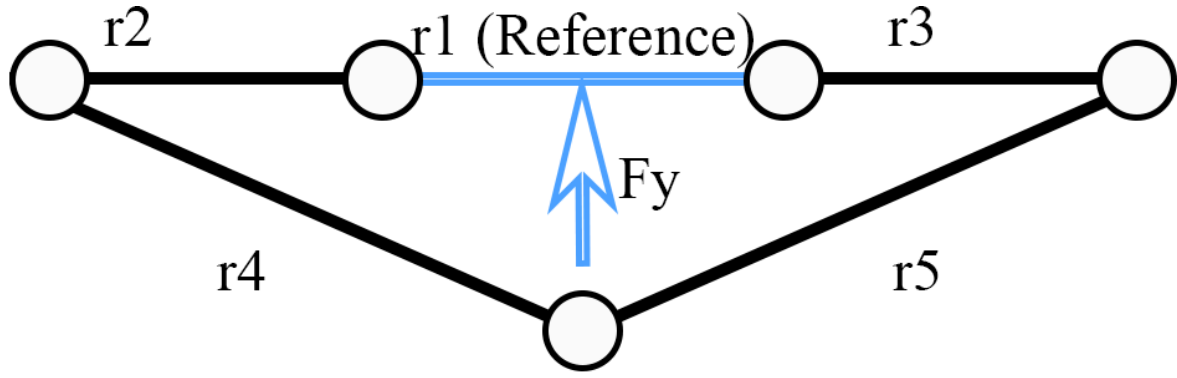


Figure 6. Force Applied on R1 with Mass

Using the new position to obtain a new set of theta 2 and theta 4 using the vector loop shown in figure x. and repeat these steps from figure 7. using a time increment of 1ms. The following diagram can be constructed as a result.

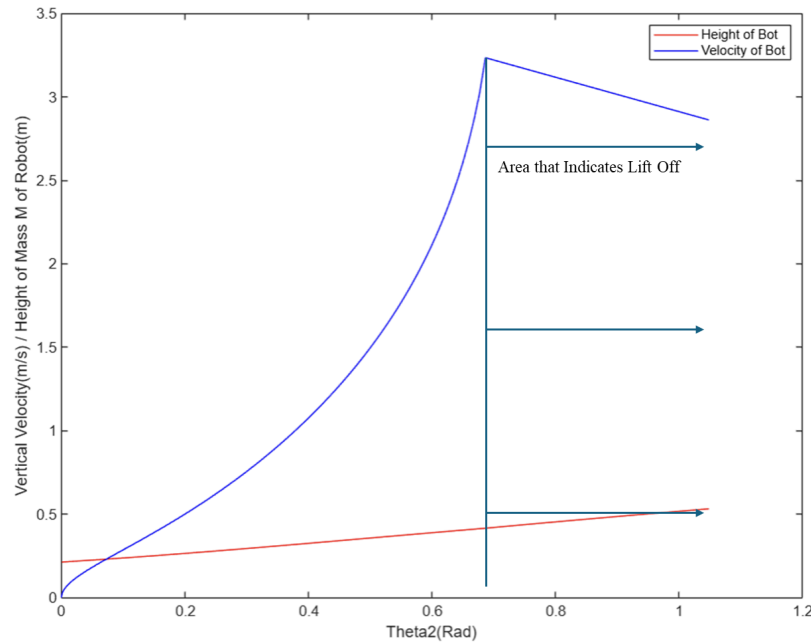


Figure 7. Vertical Velocity of Element R1

Notice how there is a sharp increase and decrease in velocity in this graph. This is because in the calculation, it is assumed that joint 45 is always held stationary to the ground which could result in a negative acceleration of the system in figure 6. In reality, this is where the robot will jump as the velocity of the leg's extension is smaller than the velocity in which the robot is traveling upward. At this point, the height of the mass is 0.4270m, and the vertical velocity is 3.2347m/s. By using the formula below to calculate the time it takes to arrive at top of the jump by setting $V_f = 0$; $V_0 = 3.2347\text{m/s}$; $g = -9.81\text{m/s}^2$

$$V_f = V_0 + gt$$

Solve the equation and find that the time it takes to travel to top of the jump is $t = 0.3297\text{s}$;

Using displacement equations.

$$D = V_0 t + gt^2/2$$

$$D = 3.2347m/s * 0.3297 - 9.81 * 0.3297^2/2 = 0.533m$$

3.3.2 Horizontal Motion

Observe from the vector loop below two equations.

$$\cos(\Theta_4) * r_4 + \cos(\Theta_2) * r_2 + 0.12 - \cos(\Theta_3) * r_3 - \cos(\Theta_5) * r_5 = 0$$

$$\sin(\Theta_4) * r_4 + \sin(\Theta_2) * r_2 - \sin(\Theta_3) * r_3 - \sin(\Theta_5) * r_5 = 0$$

By restraining the conditions for Θ_2 and Θ_3 respectively according to table x, the values of Θ_4 and Θ_5 that solves the vector loop can be obtained. Running the simulation for all assumptions and the animation shown in figure 8 below can be generated as a result.

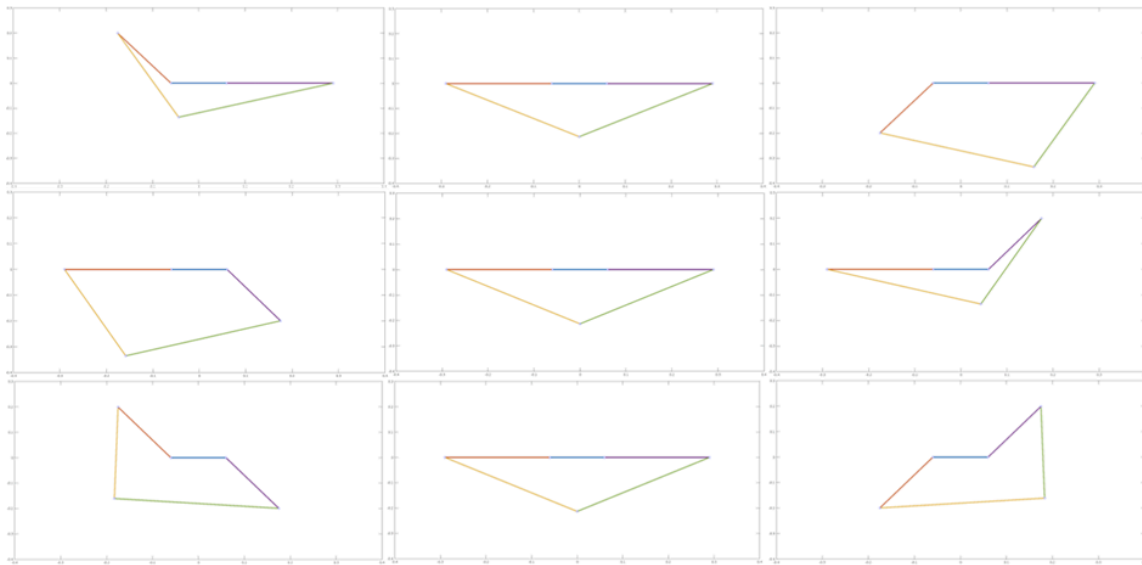


Figure 8 Joints Motion of Robot for Moving θ_2 Moving θ_3 , and Moving θ_3 & θ_2

Table 2. shows the list of horizontal distances the device can travel under these constraints.

Table 2. Range of Lower Joint Travel Under Different Constraints

	Only θ_2 moves	Only θ_3 moves	Both θ_2 and θ_3 move
Horizontal Distance (Left Limit)	0.0434m	0.1584m	0.1829m
Horizontal Distance (Right Limit)	0.1584m	0.0434m	0.1829m

By drawing the free body diagram, we can recognize that there exists a force couple between the normal force that supports the robot and the weight of the robot. This force provides a moment to the robot characterized by the equation below, where parameters are as labeled in the figure 9.

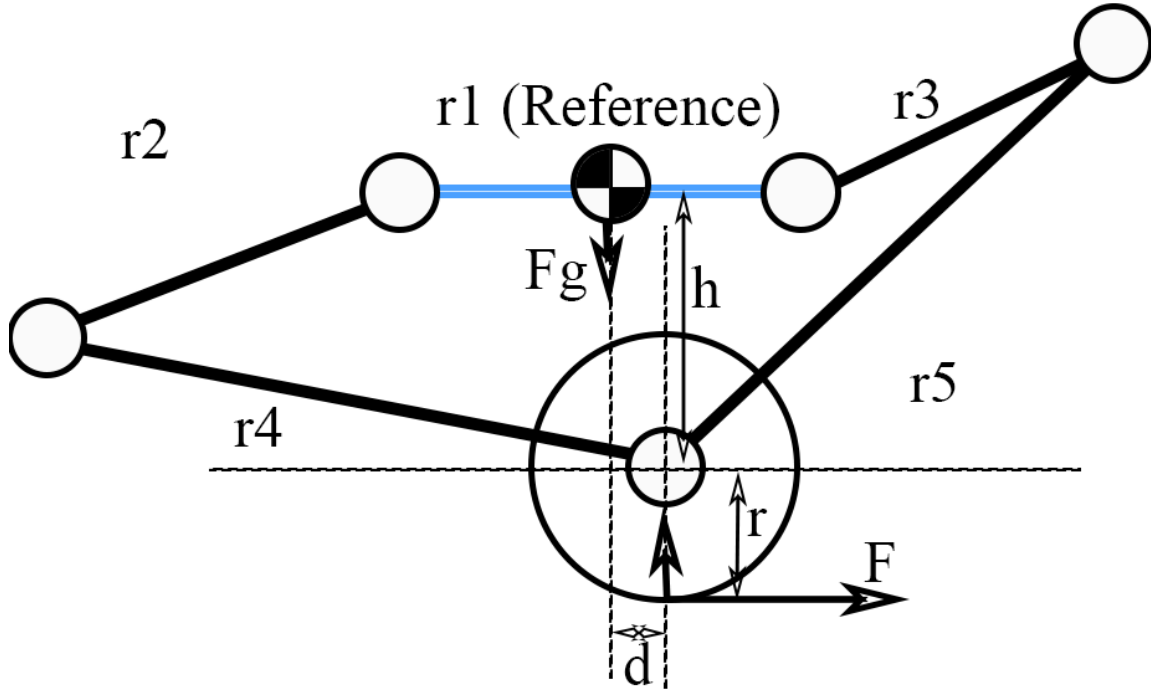


Figure 9 Free Body Diagram when the Robot Changes Speed

This is because the vertical component of the force should sum to zero when not jumping, and thus the supporting normal force equals the force of gravity.

$$M = mgd$$

Therefore, by controlling the horizontal position of the wheel relative to the center of mass, the range of moment can be obtained. When the robot is in motion, this moment will equal to the moment that results from rotating the wheel, which sums to

$$M_{Wheel} = F(h + r)$$

where F is the reaction force from the ground when the wheel rotates to accelerate the car, h is the height of the lowest joint, and r is the radius of the wheel. F can also be written as

$$F = \frac{T}{r}$$

where T is the motor torque. As $\frac{T}{r}$ calculates the action force on the ground which should be the same as the reaction force. Thus, maximum motor torque during acceleration can be written as;

$$\frac{T}{r}(h + r) = mgd$$

solve for T and get

$$T = \frac{mgdr}{h+r}$$

For the purpose of this calculation, r is set to be the radius of commercially available wheels found at [7] due to the vast amount and low pricing in Arduino Robot application, thus the following relation can be established.

$$r = \frac{65mm}{2} = 32.5mm$$

Using these formulas and parameters, the maximum acceleration and acceleration for the device can be found for all three stated constraints. Below table 3 documents the acceptable rate of acceleration and deceleration

Table 3. Range of Lower Joint Travel Under Different Constraints

	Only θ_2 moves	Only θ_3 moves	Both θ_2 and θ_3 move
Max Acceleration Torque	0.2675Nm	0.3338Nm	0.9097Nm
Max Deceleration Torque	0.3338Nm	0.2675Nm	0.9097Nm

4.0 Conclusion

In summary, this jumping robot design will be further enhancing adaptability and efficiency in search and rescue according to the mission of GRI. This hybrid approach introduces efficiency from wheels and the adaptability of legs in negotiating complex terrains based on detailed kinematic modeling, mechanism design, and performance simulation. Although there are still some trade-offs among cost, control complexity, and scalability, the robot has great potential in practical applications, including disaster response and exploratory missions. In this regard, further development of the control algorithm, coupled with mechanism refinement to enhance robustness and versatility, is necessary for practical use.

6.0 References

- [1] T. Guo et al., “Design and dynamic analysis of jumping wheel-legged robot in complex terrain environment,” *Frontiers*, <https://www.frontiersin.org/journals/neurobotics/articles/10.3389/fnbot.2022.1066714/full> (accessed Nov. 1, 2024).
- [2] Y. Zhang, L. Zhang, W. Wang , Y. Li, and Q. Zhang, “Design and implementation of a two-wheel and hopping robot with a linkage mechanism | IEEE Journals & Magazine | IEEE Xplore,” *IEEEAccess*, <https://ieeexplore.ieee.org/document/8419761/> (accessed Nov. 2, 2024).
- [3] “RC 540 Motor Brushless Motor ESC 40A 1200KV FOC sensing drive circuit RC electric motor for 1/10 RC Car,” *Amazon.ca: Toys & Games*, <https://www.amazon.ca/Brushless-1200KV-Sensing-Circuit-Electric/dp/B0DH4V3GQY/> (accessed Dec. 8, 2024).
- [4] KlimukVI, “ Wheel D65x25,” *Free CAD Designs, Files & 3D Models | The GrabCAD Community Library*, <https://grabcad.com/library/wheel-d65x25-1> (accessed Dec. 8, 2024).
- [5] A. Ives, “ SERVO ARM HORN 25T ALUMINIUM,” *Free CAD Designs, Files & 3D Models | The GrabCAD Community Library*, <https://grabcad.com/library/servo-arm-horn-25t-aluminium-1> (accessed Dec. 8, 2024).
- [6] Y. Zenichowski, “Servo SPT5435LV 35kg 180 25t,” *Free CAD Designs, Files & 3D Models | The GrabCAD Community Library*, <https://grabcad.com/library/servo-spt5435lv-35kg-180-25t-1> (accessed Dec. 8, 2024).
- [7] “4Pcs Smart Car Robot Plastic Tire Wheel DC 3V/5V/6V 65mm Diameter for Arduino Smart Car Robot,” *Amazon.com: Toys & Games*, <https://www.amazon.com/arduino-smart-Robot-Plastic-Wheel/dp/B072V3FTR6> (accessed Dec. 8, 2024).